Available online at www.sciencedirect.com

ScienceDirect

Procedia Computer Science 58 (2015) 673 – 682

Procedia Computer Science

Second International Symposium on Computer Vision and the Internet(VisionNet'15)

Image Denoising using Variations of Perona-Malik Model with different Edge Stopping Functions

V Kamalaveni [a], R Anitha Rajalakshmi[a], K A Narayanankutty[b]*

[a] *Department of Computer Science and Engineering, Amrita Vishwa Vidyapeetham, Coimbatore 641112, India*
[b] *Corporate & Industry Relations, Amrita Vishwa Vidyapeetham, Coimbatore 641112, India*

Abstract

Anisotropic diffusion is used for both image enhancement and denoising. The Perona-Malik model makes use of anisotropic diffusion to filter out the noise. In Perona-Malik model the rate of diffusion is controlled by edge stopping function. The drawback of Perona-Malik model is that the sharp edges and fine details are not preserved well in the denoised image. But the sharp edges and fine details can be preserved well using appropriate edge stopping function. We have analysed the effect of different edge stopping functions in anisotropic diffusion in terms of how efficient they are in preserving edges. We have found that an edge stopping function which stops diffusion from low image gradient onwards well preserves the sharp edges and fine details. This property of an edge stopping function will also result in lower evolution in case of level set methods. But an edge stopping function which stops diffusion from high image gradient onwards will not preserve sharp edges and fine details, since they are blurred due to diffusion. We have also found that low values of gradient threshold parameter used in edge stopping function well preserves the sharp edges and fine details than high values of threshold parameter. By utilizing an edge stopping function which stops diffusion from low image gradient onwards or which has zero or insignificant value at low image gradient, we can well preserve the sharp edges and fine details in the denoised image.

Peer-review under responsibility of organizing committee of the Second International Symposium on Computer Vision and the Internet (VisionNet'15)

Keywords: Heat Equation, Perona–Malik (PM) equation, diffusion coefficient, edge stopping function, flow function

* Corresponding author. Tel.:+91-956-661-8469
E-mail address:v_kamalaveni@cb.amrita.edu

Peer-review under responsibility of organizing committee of the Second International Symposium on Computer Vision and the Internet (VisionNet'15)
doi:10.1016/j.procs.2015.08.087

1. Introduction

Perona-Malik model which is non-linear anisotropic diffusion model proposed by Perona and Malik in 1990. It is a partial differential equation based image processing technique. Perona-Malik model can successfully remove noise while preserving edges and small structures as long as the diffusion coefficient or edge stopping function $c(|\nabla I|)$ and gradient threshold parameter (K) are estimated correctly. The gradient magnitude threshold parameter K that differentiates between image gradients due to noise and those gradients that are more likely to represent image edges. Since these are the important parameters that decides rate of diffusion, if not properly estimated will result in either over smoothed image or will leave the image with most of the noise unfiltered. Since there are several edge stopping functions, their ability to filter the noise and ability to preserve the edges when used in Perona-Malik model need to be studied and evaluated to make an appropriate choice.

2. Review of PDE Models in Image Enhancement

The first anisotropic PDE model was proposed by Perona-Malik in year 1990[1]. This model may fail when the gradient due to noise is close to gradient of image edges. So a better version of PM model was suggested by Catte in 1992[2]. In this method the image should be smoothened first by convolving with Gaussian filter then the gradient to be computed. Gabor suggested an inverse heat equation[3]. Here enhanced image is generated by subtracting its laplacian from the given image. But the reverse heat equation is an ill-posed problem. Rudin and Osher proposed a shock filter which can be used for image deblurring[4]. The shock filter makes use of a dilation process if a pixel belongs to influence zone of a maximum and an erosion process if it belongs to influence zone of minimum. Which zone the pixel belongs to that decision is taken based on the sign of the laplacian. A slightly better version of the shock filter was proposed by Kramer replacing laplacian in shock filter equation with directional second derivative of the image[5]. Weicket proposed an shock filter based on diffusion tensor[8]. Tian et al. proposed a image denoising algorithm based on difference eigenvalue[9]. Y.Q.Wang et al. suggested a modified PM model based on directional laplacian which can remove staircase effect and can preserve sharp edges[10]. Kui Liu et al. proposed an adaptive anisotropic diffusion based on structure tensor[13].

3. Overview of Perona-Malik Model

For image denoising isotropic diffusion can be used. In isotropic diffusion the rate of diffusion is uniform across all directions. Isotropic diffusion is modeled as a two dimensional partial differential equation known as Heat Equation. Denoising an image the heat equation can be solved at different instance of time t. Heat equation is described as given in eqn. (1)

$$u_t = k\Delta u = k\left(\frac{\partial^2 u}{\partial x^2} + \frac{\partial^2 u}{\partial y^2}\right) \tag{1}$$

$$u(x, y, 0) = \theta(x, y) \tag{2}$$

Where θ(x,y) is the noisy image, k=1.

In Perona-Malik model the diffusion coefficient $c(|\nabla I|)$ is a function of local image gradient. Its value is inversely proportional to the magnitude of the gradient. Since the magnitude of gradient is weak within uniform or inner regions, diffusion coefficient almost 1, so it acts as heat equation, it smoothens the inner region and removes the noise. Near boundaries the magnitude of the gradient will be strong, thereby diffusion coefficient is almost zero, so the diffusion is stopped across boundaries and it preserves the edges. Perona-Malik model is described as given in eqn. (3)

$$\frac{\partial u}{\partial t} = div(c(|\nabla u(x,y,t)|)\nabla u(x,y,t)) \tag{3}$$

$$u(x,y,0) = \theta(x,y) \tag{4}$$

Where u_t = u(x,y,t) = image obtained after a diffusion time t, *div* is the divergence operator and ∇ is the gradient operator with respect to the spatial variables x and y. $|\nabla|$ is the local gradient magnitude. And c(.) is so-called diffusion coefficient or edge stopping function.

3. Edge Stopping Functions

The edge stopping function c(s) is chosen theoretically satisfying two conditions. One is $\lim_{s\to 0}$ c(s) =1, so that rate of diffusion is high within uniform or inner regions and the other one is $\lim_{s\to\infty}$ c(s) =0, so that the diffusion is totally zero across boundaries. The important property of edge function is that they should have a zero value or insignificant value for those gradients that corresponds to edges.

Two edge stopping functions suggested by Perona and Malik [1] are given in eqn.(5) & (6)

$$c_1(|\nabla I|) = \exp\left(-\left(\frac{|\nabla I|}{K}\right)^2\right) \tag{5}$$

$$c_2(|\nabla I|) = \frac{1}{1+\left(\frac{|\nabla I|}{K}\right)^2} \tag{6}$$

where K is the gradient magnitude threshold parameter that decides the amount of diffusion to take place..

Black et.al [18] proposed a edge stopping function called Tukey's biweight function given in eqn.(7)

$$c_3(|\nabla I|) = \begin{cases} \frac{1}{2}\left[1-\left(\frac{|\nabla I|}{S}\right)^2\right]^2 & ; \ |\nabla I| \le S \\ 0 & ; \ \text{otherwise} \end{cases} \tag{7}$$

where S=K$\sqrt{2}$.

Zhichang Guo et.al [7] proposed a different edge stopping function given in eqn.(8)

$$c_4(|\nabla I|) = \frac{1}{1+\left(\frac{|\nabla I|}{K}\right)^{\alpha(|\nabla I|)}} \tag{8}$$

$$\alpha(|\nabla I|) = 2 - \frac{2}{1+\left(\frac{|\nabla I|}{K}\right)^2} \tag{9}$$

Weickert [19] proposed a edge stopping function given in eqn.(10)

$$c_5(|\nabla I|) = 1 - \exp(-3.31488 * K^8 / (|\nabla I|)^8) \quad ; \text{If} \quad (|\nabla I|) \neq 0$$

$$1 \quad ; \text{Otherwise} \tag{10}$$

The edge functions c_1, c_2, c_3, c_4 and c_5 are plotted against image gradients for threshold parameter K= 1 and 2 and the graphs looks as given in Fig.1 and Fig. 2. The graphs shows diffusion rate for different edge functions.

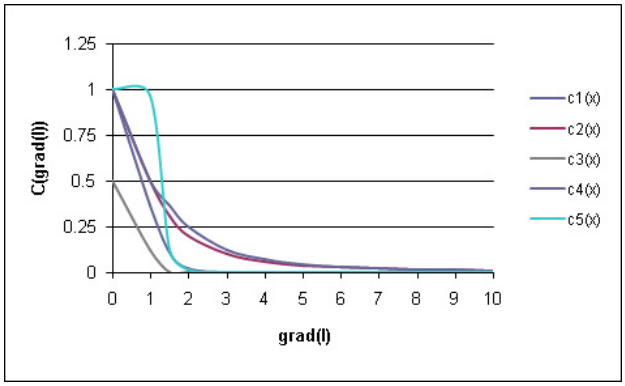

Fig 1. Edge function (amount of diffusion) versus image gradient for K=1

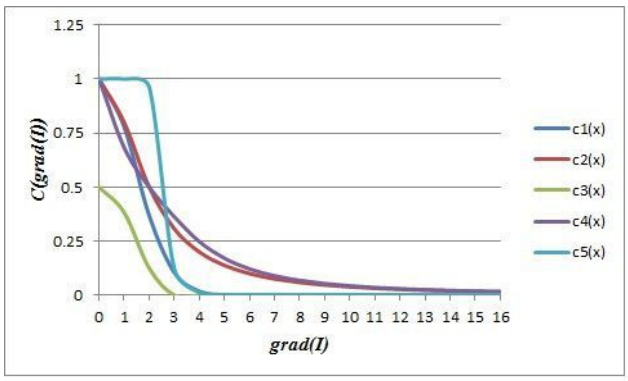

Fig 2. Edge function (diffusion) versus image gradient for K=2

As per the graph given in Fig.1 and Fig.2 the edge function c_3 stops diffusion from smaller image gradient onwards. The edge functions c_1 and c_5 stops diffusion from little higher image gradient onwards. The edge functions c_2 and c_4 stops diffusion from higher image gradient onwards. Among all edge functions c_3 is best in preserving sharp edges and fine details. Next c_1 and c_5 is good in preserving sharp edges and fine details. The edge functions c_2 and c_4 is worst in preserving sharp edges and fine details. The edge functions c_2 and c_4 has almost same diffusion rate and the edge functions c_1 and c_5 has same diffusion rate shown in Fig.1 and Fig. 2 .

The Tukey's biweight function $c_3(|\nabla I|)$ the diffusion decreases more rapidly and reaches zero, thereby it could able to protect the edges from excessive smoothing and blurring. When $c_3(|\nabla I|)$ edge function used, the resulting image will contain intact all the edges above a certain threshold (the point $|\nabla I| = S$, where $c_3(|\nabla I|)$ reaches zero). From the graph shown in Fig. 1 we conclude that all the edges where the gradient is greater than $\sqrt{2}$ are well preserved since $c_3(|\nabla I|)$ function totally stops diffusion where the gradient is greater than $\sqrt{2}$ for K=1 and S = $\sqrt{2}$. $c_3(|\nabla I|)$ function will leave those edges where the gradient is greater than $\sqrt{2}$ untouched while the other functions will not. S is treated as boundary between noise and edges in edge function c_3. Local gradients below S will be smoothed and those above S are considered as edges and diffusion totally stopped. With K=2, the edge function c_3 will leave those edges where the gradient is greater than $2\sqrt{2}$ untouched. So when c_3 function is used as edge stopping function, the Perona-Malik model will produce sharper edges.

Edge functions c_2 and c_4 stops diffusion at higher image gradient i.e eight for threshold parameter K=1 which is shown in Fig.1. So all those image pixels having gradient less than eight are diffused only image pixels having gradient greater than eight are considered as edges and not diffused. In this case sharp edges and fine details are diffused. So Perona-Malik model using either edge function c_2 or c_4 will not preserve sharp edges and fine details..

Edge functions c_1 and c_5 stops diffusion at lower image gradient i.e two for threshold parameter K=1. So all those image pixels having gradient less than two are diffused and image pixels having gradient greater than two are considered as edges and not diffused. In this case sharp edges and fine details are not diffused they are preserved. The Perona-Malik model using any of these two edge functions well preserves sharp edges and fine details.

For high values of threshold parameter, edge function stops diffusion at high image gradient. Example for threshold parameter K=2, the edge functions c_2 and c_4 stops diffusion at higher image gradient i.e 16. c_1 and c_5 stops diffusion at gradient = 4. The edge function c_3 stops diffusion at $2\sqrt{2}$. For low values of threshold parameter, the edge function stops diffusion at low image gradient. Example for K=1, the edge function c_2 and c_4 stops diffusion at gradient = 8. The edge functions c_1 and c_5 stops diffusion at gradient =2. The edge function c_3 stops diffusion at gradient $=\sqrt{2}$. So sharp edges and fine details are preserved well if threshold parameter is low.

All these findings are found to be true in our experimental results as given in table 1 and 2 and also from the visual quality of denoised images given in Fig. 3 to Fig 12.

.

4.*1 Calculating the gradient*

By using the right choice of edge stopping function, the edge preserving behaviour of Perona-Malik model can be enhanced. But it cannot denoise efficiently the images having higher amount of noise. This is because the image gradient is not a reliable measure since it is influenced by noise also. To overcome this problem, replace the term $c(|\nabla I|)$ with $c(|\nabla G_\sigma * I|)$ or $c(|\nabla I_{(x,y,t)}|)$ with $c(|\nabla(G_\sigma * I(x,y,t)|)$ where G_σ is a Gaussian filter of scale σ. This means that image should be smoothened first by convolving with gaussian filter then the gradient to be computed.

5.Denoising Performance Metrics

These are the following metrics we calculated to measure the performance of denoising with Perona-Malik model. The Peak signal-to-noise ratio (PSNR) and Mean absolute error (MAE) are defined as

$$PSNR = 10\log_{10}\left(\frac{255^2}{\frac{1}{MN}\sum_{x=0}^{M-1}\sum_{y=0}^{N-1}\left[I(x,y)-I_0(x,y)\right]^2}\right) \tag{11}$$

$$MAE = \frac{\left\|I(x,y)-I_0(x,y)\right\|_1}{MN} \tag{12}$$

where I and I_0 are original image and reconstructed image and M:N represents the size of the image respectively, in horizontal and in vertical direction. $PSNR_{grad}$ is used to measure how well derivatives of restored image match those of the original image

$$PSNR_{grad} = \frac{1}{2}\left(PSNR(\partial I_x,(\partial I_0)_x) + PSNR(\partial I_y,(\partial I_0)_y)\right)$$

(13)

6. Experimental Result

Anisotropic diffusion is implemented by solving a Perona-Malik equation using finite difference method i.e Euler forward method iteratively. Since in satellite and medical images salt and pepper noise is profound, we have synthetically added salt and pepper noise and considered the image before noise addition as reference. Denoised image using Perona-Malik model with different edge stopping functions is given in Fig. 3 to Fig. 12. The results are analysed for threshold parameter K=1,2,3,4,5 for noise density d=0.01 and 0.05 and number of iterations used is 10.

Fig 3.Threshold Parameter K=1 (a) Noisy image with salt and pepper noise density d = 0.01 (b) PM model using $c_1(x)$ (c) PM model using $c_2(x)$ (d) PM model using $c_3(x)$ (e) PM model using $c_4(x)$ (f) PM model using $c_5(x)$

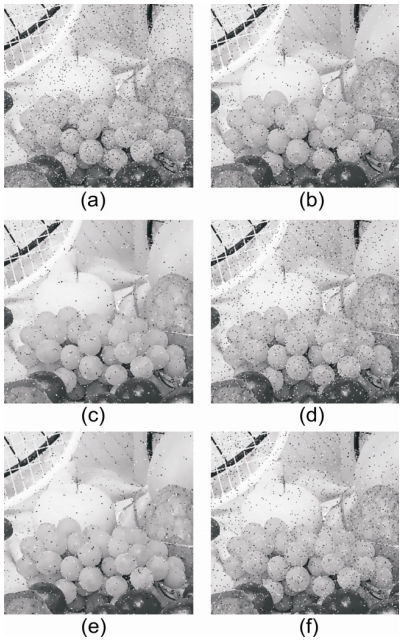

Fig 4.Threshold Parameter K=1 (a) Noisy image with salt and pepper noise density d = 0.05 (b) PM model using $c_1(x)$ (c) PM model using $c_2(x)$ (d) PM model using $c_3(x)$ (e) PM model using $c_4(x)$ (f) PM model using $c_5(x)$

Fig 5.Threshold Parameter K=2 (a) Noisy image with salt and pepper noise density d = 0.01 (b) PM model using $c_1(x)$ (c) PM model using $c_2(x)$ (d) PM model using $c_3(x)$ (e) PM model using $c_4(x)$ (f) PM model using $c_5(x)$

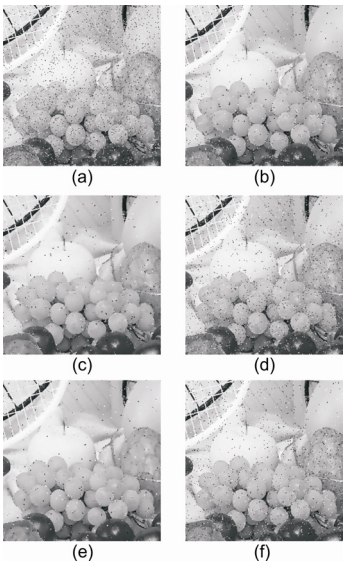

Fig 6.Threshold Parameter K=2 (a) Noisy image with salt and pepper noise density d = 0.05 (b) PM model using $c_1(x)$ (c) PM model using $c_2(x)$ (d) PM model using $c_3(x)$ (e) PM model using $c_4(x)$ (f) PM model using $c_5(x)$

Fig 7.Threshold Parameter K=3 (a) Noisy image with salt and pepper noise density d = 0.01 (b) PM model using $c_1(x)$ (c) PM model using $c_2(x)$ (d) PM model using $c_3(x)$ (e) PM model using $c_4(x)$ (f) PM model using $c_5(x)$

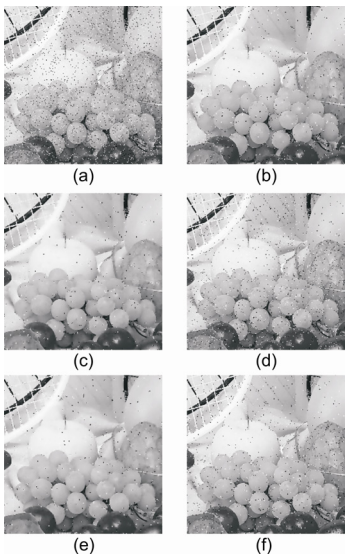

Fig 8.Threshold Parameter K=3 (a) Noisy image with salt and pepper noise density d = 0.05 (b) PM model using $c_1(x)$ (c) PM model using $c_2(x)$ (d) PM model using $c_3(x)$ (e) PM model using $c_4(x)$ (f) PM model using $c_5(x)$

Fig 9.Threshold Parameter K=4 (a) Noisy image with salt and pepper noise density d = 0.01 (b) PM model using $c_1(x)$ (c) PM model using $c_2(x)$ (d) PM model using $c_3(x)$ (e) PM model using $c_4(x)$ (f) PM model using $c_5(x)$

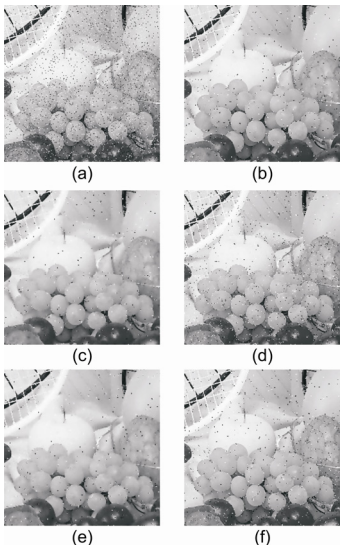

Fig 10.Threshold Parameter K=4 (a) Noisy image with salt and pepper noise density d = 0.05 (b) PM model using $c_1(x)$ (c) PM model using $c_2(x)$ (d) PM model using $c_3(x)$ (e) PM model using $c_4(x)$ (f) PM model using $c_5(x)$

Fig 11.Threshold Parameter K=5 (a) Noisy image with salt and pepper noise density d = 0.01 (b) PM model using $c_1(x)$ (c) PM model using $c_2(x)$ (d) PM model using $c_3(x)$ (e) PM model using $c_4(x)$ (f) PM model using $c_5(x)$

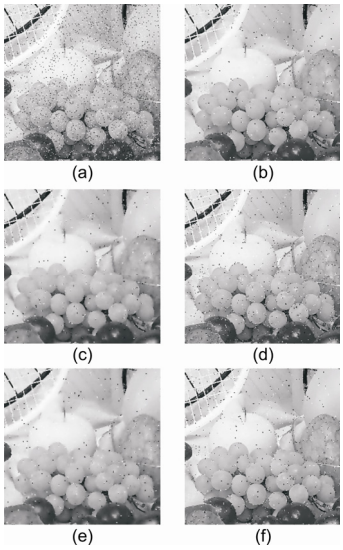

Fig 12.Threshold Parameter K=5 (a) Noisy image with salt and pepper noise density d = 0.05 (b) PM model using $c_1(x)$ (c) PM model using $c_2(x)$ (d) PM model using $c_3(x)$ (e) PM model using $c_4(x)$ (f) PM model using $c_5(x)$

Table 1. MAE, PSNR and PSNRgrad comparisons for Perona-Malik Model using edge functions $c_1(x)$, $c_2(x)$, $c_3(x)$

IMAGE	K	C1(x)			C2(x)			C3(x)		
		MAE	PSNR	$PSNR_{grad}$	MAE	PSNR	$PSNR_{grad}$	MAE	PSNR	$PSNR_{grad}$
Lena	1	0.9060	31.1102	68.5993	2.5614	27.6854	65.3189	0.2496	35.4459	76.1807
(d=0.01)	2	2.0567	28.1855	64.0678	4.0478	26.3529	61.8527	0.7765	30.9170	69.7363
	3	3.0142	27.0414	61.6505	5.2330	25.6761	60.1942	1.2304	29.5389	67.5008
	4	3.8720	26.2828	60.4535	6.2508	24.9465	58.5107	1.5834	29.1165	65.9362
	5	4.5765	25.8986	58.7664	7.4453	24.2536	56.8188	2.0367	28.0319	64.0963
Fruits	1	2.6601	23.1217	69.3803	5.3941	20.8348	61.5826	0.7617	28.3547	80.9519
(d=0.05)	2	4.3256	21.3689	62.8061	6.9956	19.9801	57.8149	2.1504	23.9271	63.2403
	3	5.6305	20.3381	56.1560	8.1664	19.5675	56.4114	2.9157	22.9570	62.4575
	4	6.2673	20.1107	54.2064	9.2137	19.0705	54.4471	3.8878	21.6369	60.6457
	5	7.0978	19.6224	51.7109	10.1797	18.8636	51.3288	4.5375	21.0800	57.9668

Table 2. MAE, PSNR and PSNRgrad comparisons for Perona-Malik Model using edge functions $c_4(x)$, $c_5(x)$

IMAGE	K	C4(x)			C5(x)		
		MAE	PSNR	$PSNR_{grad}$	MAE	PSNR	$PSNR_{grad}$
Lena	1	2.5817	28.0753	64.8342	0.6225	31.6393	70.6120
(d=0.01)	2	4.2337	26.0960	61.9903	1.4261	29.3179	65.7914
	3	5.4747	25.5137	59.6352	2.2172	28.0046	63.1795
	4	6.8580	24.8650	57.4594	2.9458	27.1420	61.0730
	5	7.5340	24.3120	56.7846	3.5315	26.7623	60.1242
Fruits	1	5.4505	20.8222	62.1817	1.7207	24.9418	67.4862
(d=0.05)	2	7.1569	19.8492	59.0337	3.4312	22.1489	66.2755
	3	8.4845	19.2171	56.7888	4.5548	21.0994	58.3571
	4	9.2839	19.0654	53.8955	5.2691	20.7586	57.3813
	5	9.8827	18.8793	51.9616	6.1052	20.0530	56.5315

6. Conclusion

Comparing the quality metrics calculated for different edge functions, PSNR values are high for Perona-Malik model using edge function c_3. Since for c_3 the diffusion reduces more rapidly and totally stops diffusion where the gradient is very minimum. The sharp edges and fine details are well preserved hence its PSNR is high. Also from the visual quality of the restored image the above fact is found to be true. Among all edge functions c_3 function is very efficient in preserving sharp edges and fine details. For c_2 and c_4 the values of quality metric PSNR are very close and differ by a small value but is less compared to PSNR values of c_1, c_3 and c_5. From both the visual quality of the restored images as well as based on PSNR values, it is found that c_2 and c_4 are not efficient in preserving sharp edges and fine details.. The PSNR values of c_1 and c_5 are greater than the PSNR values of c_2 and c_4. From the visual quality of the restored images and also from PSNR values, c_1 and c_5 are found to be good in preserving sharp edges and fine details. Performance of Perona-Malik model using c_5 is little higher than performance of Perona-Malik model using c_1. Also increase in K results in loss of more fine details. This is found to be true in our experimental results since for all edge stopping functions, increase in K causes decreases in PSNR value. By making right choice of edge stopping function and gradient threshold parameter the sharp edges and fine details can be well preserved in Perona-Malik model.

References

[1] Pietro Perona and Jitendra Malik, Scale-Space and Edge Detection Using Anisotropic Diffusion, *IEEE Transactions on Pattern Analysis and Machine Intelligence*, July 1990, VOL. 12, No2.

[2] F. Catte, P.L.Lions, J.M.Mortel, et al., Image selective smoothing and edge detection by nonlinear diffusion,.SIAM J, Numerical Analysis, vol.29,no. 1,pp. 182-193, Feb. 1992.

[3] M.Lindenbaum, M.Fischer, and A.M.Bruckstein, On gabor's contribution to image enhancement, Pattern Recognition, vol. 27, no.1, pp 1-8, Jan. 1994.

[4] S.Osher and L.I. Rudin, "Feature-Oriented image enhancement using shock filter, SIAM J , Numerical Analysis, vol.27, no.4, pp 919-940, Aug.1990.

[5] H P Kramer and J.B.Bruckner,Iterations of a non-lineartransformation for enhancement of digital images, Pattern Recognition, vol.7, no 1-2, pp 53-58, June.1975.

[6] Guo W. Wei, Generalized Perona–Malik Equation for Image Restoration, *IEEE Signal Processing Letters*, JULY 1999, VOL. 6, NO. 7.

[7] Zhichang Guo, Jiebao Sun, Dazhi Zhang and Boying Wu, Adaptive Perona–Malik Model Based on the Variable Exponent for Image Denoising , *IEEE Transactions On Image Processing*, Vol. 21, No.3, March 2012.

[8] Joachim Weicket, Coherence Enhancing diffusion Filtering, International journal of Computer Vision, 1999, 31(2-3): 111-127.

[9] H. Tian, H. Cai, J.H. Lai, et al. Effective image noise removal based on difference eigen value, In 18th IEEE International Conference on Image Processing 2011,3357-3360. .

[10] Wang Y.Q., JichangGuo, WufanChen and Wenxue Zhang, Image denoising using Modified Perona–Malik Model based on Directional Laplacian, *Signal Processing* 93 (2013) 2548–2558.

[11] Risheng Liu, Zhouchen Lin, Wei zhang, Kewei Tang and Zhixun Su, Toward desgining intelligent PDEs for computer vision: An optimal control approach, *Image and vision computing* (2013) 43-56.

[12] L.I.Rudin, S.Osher, E.Fatemi, Nonlinear total variation based noise removal algorithms, Physica D: Nonlinear Phenomena, 1992, 60(1), 259-268..

[13] Kui Liu, Jieqing Tan, Benyue Su, Adaptive anisotropic diffusion for image denoising based on structure tensor, International Conference on Digital Home, 2014..

[14] Y.L.You, M.Kaveh, Fourth-order partial differential equations for noise removal, IEEE Transcations on Image Processing, 2000, 9(10), 1723-1730.

[15] Chourmouzios Tsiotsios, Maria Petrou, On the Choice of the Parameters for Anisotropic Diffusion in Image Processing, *Pattern Recognition*, 2012.

[16] LinaSeptiana, Kang-Ping Lin, X-ray Image Enhancement using a Modified Anisotropic Diffusion, *IEEE International Symposium on Bioelectronics and Bioinformatics*, 2014.

[17] Aleksandra Pizurica, Iris Vanhamel, HichemSahli, Wilfried Philips and AntonicsKatartzis, A Bayesian formulation of edge-stopping function in non-Linear Diffusion, *IEEE Signal Processing Letters*, February 16, 2006.

[18] Black M.J., G.Sapiro, D.Marimont, D.Heeger, Robust anisotropic diffusion, *IEEE Transcations on image Processing*, March 1998, Vol 7, No 3.

[19] J.Weickert, Anisotropic diffusion in image processing, ser. ECMI Series. Stuttgart, Germany:Teubner-Verlag. 1998.

[20] Yan-Fei Zhao, Qing-Wei Gao, De-Xiang Zhang and Yi-Xiang Lu, Medical X-Ray Image Enhancement Based on Kramer's PDE Model, Journal of electronic science and technology of china, vol.5, No.2, June 2007.